Focusing enhanced broadband metalens via height optimization*

WANG Junjie, CHEN Deli, WANG Zhan, XUE Qi, and SUN Xiaohong****

Henan Key Laboratory of Laser and Opto-electric Information Technology, School of Information Engineering, Zhengzhou University, Zhengzhou 450001, China

(Received 11 June 2021; Revised 19 August 2021)

Metalenses are two-dimensional planar metamaterial lenses, which have the advantages of high efficiency and easy integration. Based on the method of spatial multiplexing, a metalens with a wide working waveband is designed by arranging TiO_2 nanopillars under the resonance phase regulation. In addition, choosing an assistant metalens with optimized heights is effective to enhance metalens's focusing, which is also illustrated in this paper. The metalens, designed with numerical aperture (*NA*) of 0.72 and center working wavelength of 600 nm, achieves the working waveband of 550—660 nm, the focus point's size of below 420 nm, and the focusing efficiency of more than 30%.

Document code: A **Article ID:** 1673-1905(2022)02-0072-5

DOI https://doi.org/10.1007/s11801-022-1095-9

In the past decade, metasurface, the one developing from three-dimensional metamaterial, has catered to the demand of high integration, and then, attracted a large number of researchers' attention as a hot pot[1-3]. Its ability to flexibly regulate electromagnetic waves is achieved by manually designing the arrangement of unit structures with sub-wavelength order on a 2D plane[4]. Specifically, the uniqueness of metasurfaces can be manifested as focusing by ultra-thin plana, absorbing or filtering with frequency selectivity, and so on. Among them, the earliest metasurfaces are microlenses called metalenses, which are one type of crucial optical devices. Metalens was firstly designed in 2012 by arranging V-shaped metal antennas under the plasma effects[5]. But plasma metalenses are inefficient due to the ohmic loss of metal[6]. In 2015, silicon metalenses realized meliorative focusing in the infrared band because of well avoiding the metal's ohmic loss[7]. Next year, new dielectric metalenses based on TiO_2 material could be equivalently efficient as silicon one, but in the visible band[8,9]. Recently, reducing the chromatic aberration and making metalenses work in multi-band[10] or wide-band[11], have become one of research directions to improve the performance of the lens. Except that, metalenses with complex and unusual functions, such as focusing at multi-point, polarization-selected focusing and tunable focusing, are emerging in a large number[12-14].

In this paper, a metalens with 600 nm as center working wavelength is designed firstly, whose working waveband is 550—630 nm. Then, a wider working waveband 550—660 nm is obtained by multiplexing it with another height-optimized metalens, one with 650 nm as the center working wavelength.

For insensitive to polarization, especially left or right circularly polarization, cylindrical TiO_2 nanopillar is chosen as the unit structure, shown in Fig.1, where *a* is the lattice period, *h* is the height and *r* is the radius of the nanopillar[15]. The nanopillar can be considered as a Fabry-Perot resonator[16]. By changing its height and radius, the resonance of electromagnetic waves in the nanopillar can be changed, so as to transform the phase of transmitted electromagnetic wave[17].

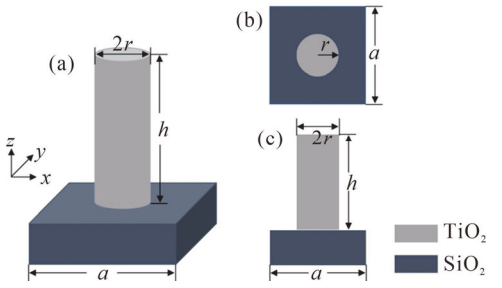

Fig.1 Unit structure of cylindrical TiO_2 nanopillar: (a) 3D view; (b) Vertical view; (c) Front view

In order to make the nanopillars as low as possible, obtain good traversal of transformed phase on [−π, π] and achieve high enough transformed efficiency, *a* is optimized to 260 nm and *h* is fixed to 650 nm, with left-hand circularly polarized light at the wavelength of 600 nm illuminating from the bottom of TiO_2. Then, the transformed efficiency and phase varies with *r*, varying as

* This work has been supported by the Science and Technology Major Project of Henan Province (No.161100210200).

** E-mails: ieqxue@zzu.edu.cn; iexhsun@zzu.edu.cn

shown in Fig.2, simulated in COMSOL Multiphysics 5.4.

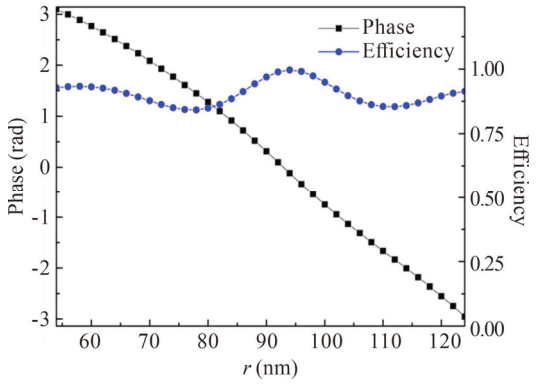

Fig.2 Transformed efficiency and phase varying with *r*, *r* traveling from 54 nm to 124 nm in steps of 2 nm

If the function of focusing is wanted, the transformed phase φ of nanopillars making up the metalens, should satisfy

$$\varphi(d,\lambda)=\frac{2\pi}{\lambda}\left[f-\sqrt{d^2+f^2}\right], \tag{1}$$

where $d=\sqrt{x^2+y^2}$ is the position of every nanopillar, λ is the wavelength of incident light, and f is the designed focal length.

Half of the metalens model is illustrated by Fig.3. That means, 40 nanopillars on a line are used to focus the incident light and the focal length is 5 μm, while the 20 nanopillars' sizes and positions are given in Tab.1, and this metalens is named as Metalens1.

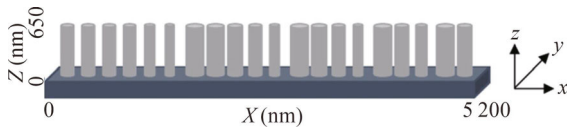

Fig.3 Half of Metalens1 model

The other 20 nanopillars can be obtained by rotating the 20 nanopillars in Fig.3 for 180° along the *Z* axis.

Tab.1 Sizes and positions of nanopillars in Fig.3

X (nm)	r_1 (nm)	*X* (nm)	r_1 (nm)	*X* (nm)	r_1 (nm)	*X* (nm)	r_1 (nm)
130	92	1 430	66	2 730	72	4 030	118
390	92	1 690	124	2 990	122	4 290	96
650	88	1 950	112	3 250	106	4 550	78
910	84	2 210	100	3 510	90	4 810	122
1 170	76	2 470	88	3 770	68	5 070	100

In Tab.1, the *X*, center coordinate of every nanopillar on *x* axis, can be expressed as (*k*−0.5)**a*, where *k* is the number of nanopillar, traveling from 1 to 20. The *Y* coordinates of nanopillars are the same 0 nm and the nanopillars' bottom coordinates *Z* are the same 0. The focusing characteristic of the Metalens1 is investigated at the incident wavelength of 550—630 nm, in which the electric energy density for the 600 nm light incidence is offered in Fig.4.

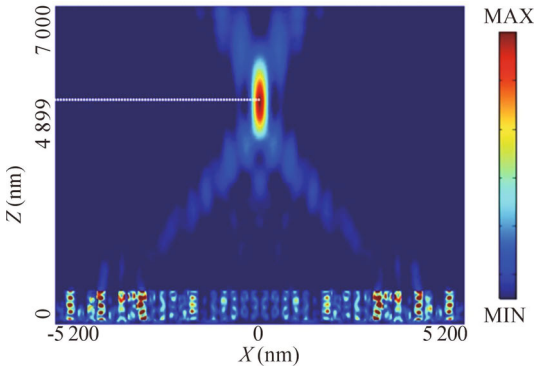

Fig.4 Electric energy intensity of Metalens1

Obviously, the focal length at the center working wavelength 600 nm is 4 899 nm, that is, the error is −2%. Besides, the focal length decreases with the increase of incident wavelength. If the working waveband is assumed as the band with error within ±10%, the down boundary of working wavelength is 550 nm with the focal length of 5 423 nm, while, the up boundary is 630 nm with the focal length of 4 512 nm. In addition, the full widths at half maximum (*FWHM*) of the focal point are below 340 nm, near the limit of resolution (half wavelength).

For a wider working waveband, multiplexing Metalens1 with an assistant metalens is an available approach. The chosen assistant metalens, Metalens2, is designed with optimized nanopillars' heights, the same 720 nm, and its focal length at the incident wavelength of 650 nm is set to 5 μm. Its focusing characteristic is also good, comparable to that of Metalens1. The nanopillars' sizes and positions can be obtained through the same approach with Metalens1. The optimization of height can avoid the transformed phase's reverse as shown in Fig.5. The reverse leads to the change of phase's varying rate, phase varying slow before the reverse while phase varying fast after the reverse. In other words, transformed phase varies fluently after the optimization and has better performance on wave control, similar to that in Fig.2.

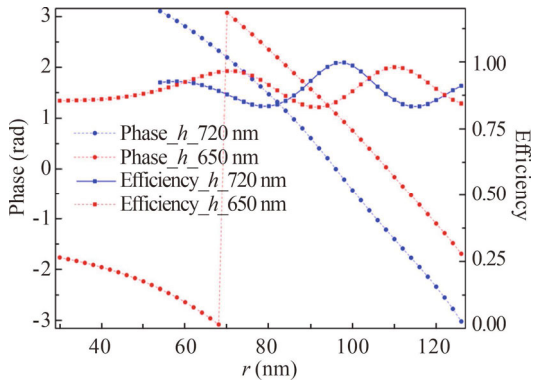

Fig.5 Effect of optimization

Then, the combine process of Metalens3, the combine process of the broadband metalens based on the method of spatial complexing, given in Fig.6, illustrates that half of nanopillars in Metalens1 and half of nanopillars in Metalens3 combines into Metalens3. In another word, Metalens1 is converted to Metalens3 when half of the nanopillars in Metalens1, the even numbered 20, are replaced by the even-numbered nanopillars in Metalens2. The focusing performance of Metalens3 is compared with another combined metalens whose assistant metalens's nanopillars' heights are unoptimized 650 nm, and both of them can be found distinctly in Fig.7. In Fig.7(a), the unoptimized one can almost focus the incident light and the undesired stray light can be observed evidently, however, in Fig.7(b), the optimized one still performs satisfyingly. It proves that it is a potential way to enhance the focusing of metalenses via height optimization. The nanopillars' sizes and positions of the two combined metalenses, are listed in Tab.2. The r_1 values in Tab.2 are parts of nanopillars' radii of the unoptimized combined metalens and the same height is 650 nm. The r_2 values in Tab.2 are parts of nanopillars' radii of Metalens3 and the same height is 720 nm. The unoptimized metalens and Metalens3 are got by substituting nanopillars in Tab.1 with those in Tab.2, respectively.

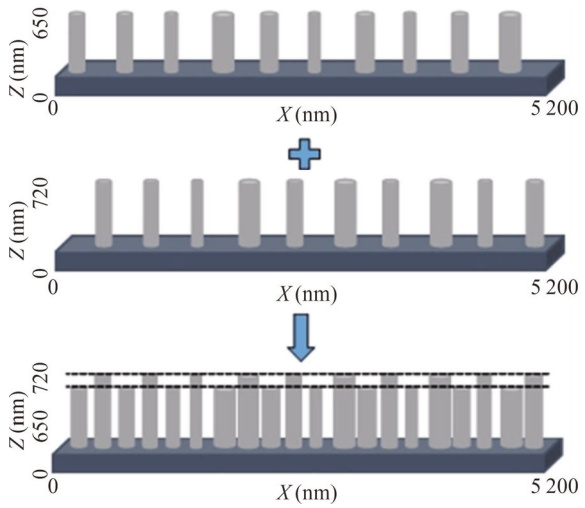

Fig.6 Combination processes of 10 nanopillars in Metalens1 and 10 nanopillars in Metalens2

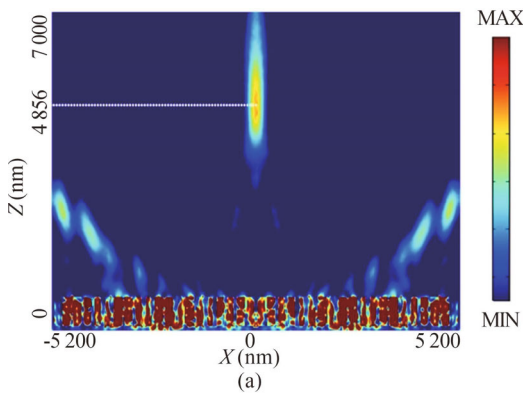

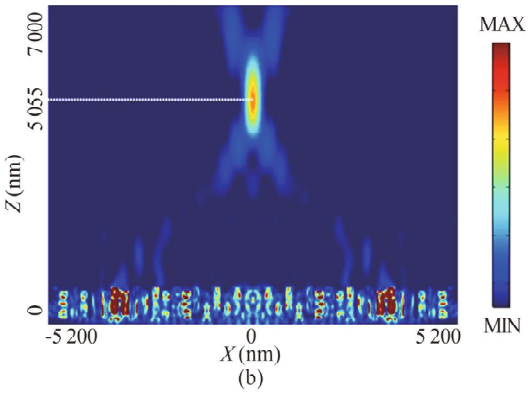

Fig.7 Enhanced focusing characteristics at the incident wavelength of 600 nm: (a) Electric energy density of the unoptimized combined metalens; (b) Electric energy density of Metalens3

Tab.2 Nanopillars' positions and sizes of the unoptimized metalens and Metalens3

X (nm)	r_1 (nm)	r_2 (nm)	X (nm)	r_1 (nm)	r_2 (nm)
390	106	94	2 990	80	60
910	98	86	3 510	118	100
1 430	82	70	4 030	82	58
1 950	54	118	4 550	114	94
2 470	110	94	5 070	70	120

The broadening of working bandwidth is evidenced in Fig.8. It presents that the working waveband of Metalens1 is 80 nm, while that of Metalens3 is 110 nm. In addition, the focal length of Metalens3 at the incident wavelength of 660 nm is 4 489 nm, very close to the boundary 4 500 nm so that 660 nm is also considered to be within working waveband. The *FWHM* of Metalens3 is below 420 nm.

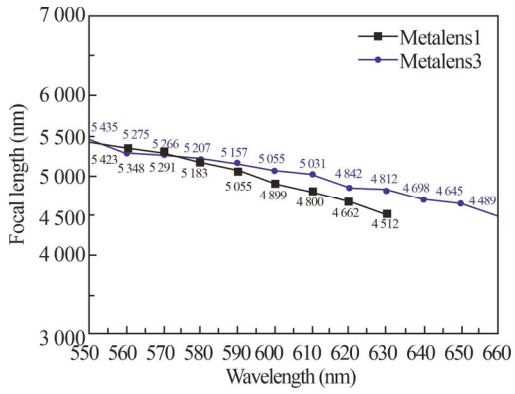

Fig.8 Focal lengths of Metalens1 and Metalens3

The reason why the working bandwidth is broadened is explained as the effect of spatial multiplexing, that is, superposition of focusing characteristics results from addition of structures. Specifically speaking, by analyzing the electric energy density along z axis, the Z coordinate

corresponding to the maximum of the curve is the focal length. The focal length of Metalens1 may be smaller than that of Metalens2 at the incidence of wave with a proper wavelength, such as 650 nm, shown in Fig.9(a). Then, the addition of transformation on incident wave, called calculational value in Fig.9(b), is got by summing the two curves of Fig.9(a) and is the assumed consequence of spatial multiplexing. The calculational focal length is located at 4 645 nm, between 4 320 nm of Metalens1 and 4 848 nm of Metalens2. The simulated focal length value of Metalens3 is pleasantly consistent with the calculational one, performing like the two curves in Fig.9(b).

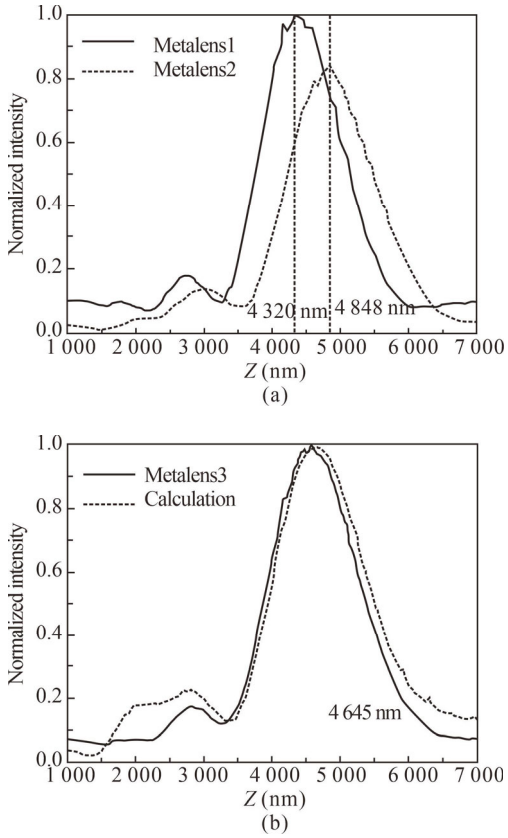

Fig.9 Addition of electric energy density along *z* axis: (a) Normalized intensities of Metalens1 and Metalens2; (b) Calculational and simulated values of Metalens3

Another evaluation parameter is focusing efficiency, the proportion of focal energy in the total incident energy[18,19]. The incident wave's electric energy density along the *X* axis in Fig.10(a) is almost a constant. So, the total incident energy is easy to get. However, the electric energy density along *X* axis at *Z* coordinate is equal to focal length. 1/10 of the peak is chosen as the boundary of focus point, and the total energy between up and down boundaries is thought as energy of focus point. In fact, expansion of working bandwidth is achieved at the cost of focusing efficiency, clearly observed in Fig.10(b), but finite and acceptable.

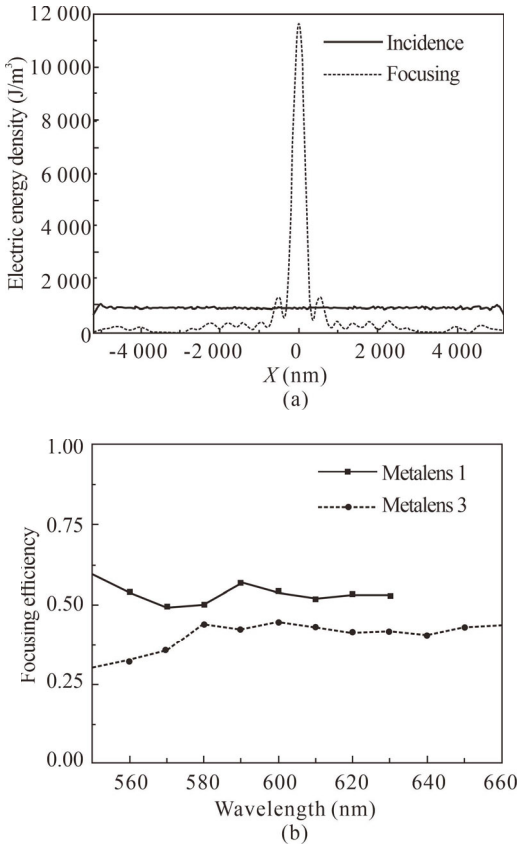

Fig.10 Evaluation of focusing efficiency: (a) Electric energy density of focus point and incident port; (b) Focusing efficiency

In this paper, the metalens whose center working wavelength is 600 nm, is designed under the guidance of resonance phase regulation. Its working bandwidth is expanded from 550—630 nm to 550—660 nm through multiplexing with another assistant metalens. Besides, the focusing is enhanced via optimizing the assistant one's nanopillars' height. Then, the mechanism of waveband's expanding is illustrated. This work reveals spatial multiplexing with an optimized assistant metalens is an available and efficient approach to improve metalens's performance, specifically on working waveband's widening and focusing enhancing. This advanced broadband metalens may be a good choice to be applied in micro optical system. Exactly, the developing optical chip is requiring these micro and efficient devices, besides, asking more.

Statements and Declarations

The authors declare that there are no conflicts of interest related to this article.

References

[1] PATRICE G, FEDERICO C, FRANCESCO A, et al. Recent advances in planar optics：from plasmonic to dielectric metasurfaces[J]. Optica, 2017, 4(1)：139-152.

[2] YU N F, FRANCESCO A, PATRICE G, et al. A broadband, background-free quarter-wave plate based on plasmonic metasurfaces[J]. Nano letters, 2012, 12(12)：6328-6333.
[3] YU N F, FEDERICO C. Flat optics with designed metasurfaces[J]. Nature materials, 2014, 13(2)：139-150.
[4] YU N F, PAREICE G, MIKHAIL A, et al. Light propagation with phase discontinuities：generalized laws of reflection and refraction[J]. Science, 2011, 334(6054)：333-337.
[5] NINA M, WILLIAM L B, LAN R H, et al. Plasmonic meta-atoms and metasurfaces[J]. Nature photonics, 2014, 8(12)：889-898.
[6] SAMAN J, ZUBIN J. All-dielectric metamaterials[J]. Nature nanotechnology, 2016, 11(1)：23-36.
[7] AMIR A, YU H, MAHMOOD B, et al. Dielectric metasurfaces for complete control of phase and polarization with subwavelength spatial resolution and high transmission[J]. Nature nanotechnology, 2015, 10(11)：937-943.
[8] MOHAMMADREZA K, CHEN W T, ROBERT C D, et al. Metalenses at visible wavelengths：diffraction-limited focusing and subwavelength resolution imaging[J]. Science, 2016, 352(6290)：1190-1194.
[9] WANG S M, CHEN D L, SUN X H, et al. GaP-based high-efficiency elliptical cylinder metasurface in visible light[J]. Chinese physics letters, 2020, 37(5)：057801.
[10] FRANCESCO A, MIKHSIL A K, PATRICE G, et al. Multiwavelength achromatic metasurfaces by dispersive phase compensation[J]. Science, 2015, 347(6228)：1342-1345.
[11] WANG S M, CHEN M K, CHEN B H, et al. A broadband achromatic metalens in the visible[J]. Nature nanotechnology, 2018, 13(3)：227-232.
[12] CHEN D L, QI Y L, SUN X H, et al. Design of dielectric deflecting metasurface and metalens in the visible-light range[J]. Optical engineering, 2021, 60(3)：035104.
[13] PAN W, WANG X Y, CHEN Q, et al. Design of multi-channel terahertz beam splitter based on Z-shaped metasurface[J]. 2020, 16(6)：437-440.
[14] CHEN D L, WANG J J, SUN X H, et al. The bifocal metalenses for independent focusing of orthogonally circularly polarized light[J]. Journal of physics D：applied physics, 2021, 54(7)：075103.
[15] CHEN D L, WANG J J, SUN X H, et al. Polarization-insensitive dielectric metalenses with different numerical apertures and off-axis focusing characteristics[J]. Journal of the optical sociery of America B, 2020, 37(12)：3588.
[16] WANG S M, CHEN D L, SUN X H, et al. The investigation of height-dependent meta-lens and focusing properties[J]. Optics communications, 2019, 460(1)：125129.
[17] LIU Y, YANG H H, LU Y L, et al. A whispering gallery mode strain sensor based on microtube resonator[J]. Optoelectronics letters, 2021, 17(4)：199-204.
[18] REZA K, SHI Z J, CHEN W T, et al. Achromatic metalens over 60 nm bandwidth in the visible and metalens with reverse chromatic dispersion[J]. Nano letters, 2017, 17(3)：1819-1824.
[19] CHEN W T, SHI Z J, FEDERICO C, et al. A broadband achromatic metalens for focusing and imaging in the visible[J]. Nature nanotechnology, 2018, 13(3)：220-226.